Yu, A. W., D. J. Harding, and P. W. Dabney. 2016. "Laser transmitter design and performance for the slope imaging multi-polarization photon-counting lidar (SIMPL) instrument." Solid State Lasers XXV: Technology and Devices, Proceedings of SPIE 9726: [10.1117/12.2213005].

Description of the instrument, including the transmitter, receiver and electronics, used for the 2015 Greenland campaign and examples of preliminary results.

Laser Transmitter Design and Performance for the Slope Imaging Multi-polarization Photon-counting Lidar (SIMPL) Instrument

Anthony W. Yu*, David J. Harding, Philip W. Dabney
NASA Goddard Space Flight Center, Greenbelt, MD, USA 20771

ABSTRACT

The Slope Imaging Multi-polarization Photon-counting Lidar (SIMPL) is a polarimetric, two-color, multi-beam push broom laser altimeter developed through the NASA Earth Science Technology Office Instrument Incubator Program. It has flown successfully on multiple airborne platforms beginning in 2008.[1] It was developed to demonstrate new altimetry capabilities that combine height measurements and information about surface composition and properties. In this talk we will discuss the laser transmitter design and performance and present recent science data collected over the Greenland ice sheet and arctic sea ice in support of the second NASA Ice Cloud and land Elevation Satellite (ICESat-2) mission to be launched in 2017.[2]

Keywords: Solid-state laser, Airborne altimetry instrument, Space lidar instrument

1. INSTRUMENT DESCRIPTION

1.1 Overview

The functional block diagram of the SIMPL instrument is shown in Figure 1(a). The instrument design is mono-static with the transmit and receive signals sharing a common telescope as illustrated in Figure 1(b). It is based on the earlier successfully flown Cloud Physics Lidar (CPL) instrument developed at Goddard Space Flight Center.[3] The SIMPL laser transmitter is a high repetition rate (~11 kHz), short-pulse (~1 ns), linearly polarized microchip laser centered at 1064 nm. Part of the near infrared (NIR) beam at 1064 nm is frequency doubled to 532 nm (Green). Each of the NIR and Green beams is split into four push-broom beams forming four parallel tracks in the flight direction. The output of the SIMPL instrument has 4 linearly polarized beams each with co-aligned wavelengths in order to have co-incident NIR and Green footprints at the surface. The 4-beam swath spans a width of ~6 to 7 mrad with equally spaced beams as illustrated in Figure 2. All transmitted beams have the same state of polarization (SOP) when projected to the ground. A 20-cm-diameter off-axis parabola (OAP) is used as the telescope primary to collect the return signal. The OAP provides a rugged and robust design that minimizes obscurations of both the outgoing and the incoming beams. None of the outgoing transmitted light is lost to obscurations, and only approximately 20% of the receiver aperture is obscured. The return signal collected by the telescope is separated into wavelength components by use of a dichroic filter.

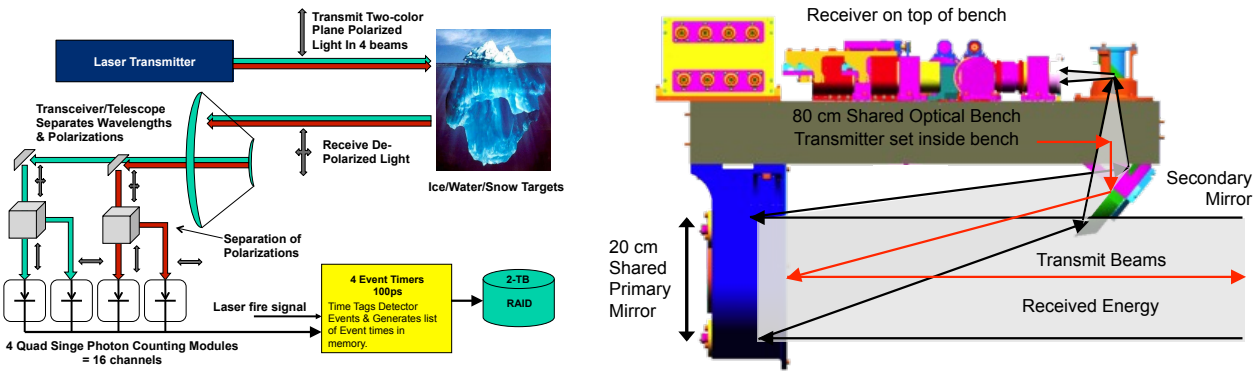

(a) (b)

Figure 1. (a) SIMPL instrument functional block diagram. (b) The SIMPL instrument transceiver has a common optical bench that houses a primary OAP and secondary mirrors that is shared by the transmitter and receiver. This design provides stable laser footprint to receiver field of view alignment, co-aligned NIR and green transmit beams and co-incident NIR and green footprints.

*anthony.w.yu@nasa.gov; phone 1 301 614-6248

Solid State Lasers XXV: Technology and Devices, edited by W. Andrew Clarkson, Ramesh K. Shori, Proc. of SPIE Vol. 9726, 97260J · © 2016 SPIE · CCC code: 0277-786X/15/$18 · doi: 10.1117/12.2213005

The receiver dichroic filter divides the two wavelengths into separate paths which are further divided using polarizing beam splitting cubes into signals parallel and perpendicular to the transmit beam, producing 16 channels (four color/polarization states on the four beams). The received light is fiber coupled into sixteen single-photon counting modules (SPCM) and timing electronics with 0.1 nsec precision are used to determine range to the target. The short pulse width and high timing precision achieves an 8 cm range precision per single detected photon. Upon aggregation of the signal photons into a range histogram a measurement with a few cm resolution of pulse broadening is achieved. The broadening is due to surface slope and roughness and for snow, ice and water light transmission into the target resulting in volume scattering.

This design was developed to meet instrument system requirement and flow-down requirements, established at the beginning of the project, needed to achieve the SIMPL measurement objectives. The high-level transmitter and receiver subsystems requirements are summarized in Table 1.

Table 1. Summary of the SIMPL instrument system and subsystems requirements.

System Requirements – • 4 cross-track spots illuminated by plane polarized Green (532 nm) and NIR (1064 nm) light • <10 cm single shot range resolution and accuracy • Eye-safe energies at aircraft separation distances (<2,000 ft) • ~0.1 to 0.3 probability of detection (PD) from 2.5 to 5 km Above Ground Level (AGL) • >10 photon samples / meter in-track for each of the 16 channels	
Laser Requirements -	
Pulse Repetition Frequency (PRF)	11 kHz
Pulse Energy	532 nm: 0.1 to 0.2 µJ per beam; 1064 nm: 0.8 – 1.1 µJ per beam
Wavelengths	532 nm and 1064 nm
Polarization Contrast	>100:1
Pulse Width	< 1 nsec
Output beam pattern	Each color has 4 beams forming parallel tracks with full separation in the cross track direction of ~6 mrad (~2 mrad between beams). Beam divergence ~130 µrad. 532 and 1064 nm beams overlap each other.
Receiver Requirements -	
Photon Detection Efficiency (PDE)	>40% PDE at visible wavelength; >3% PDE at 980-1100nm wavelength
Timing error	< 0.33 ns (5cm) single shot
Dark count	$< 2 \times 10^5$/s
Maximum count rate	$5\text{-}10 \times 10^6$/s
IFOV (Each beam/Each color)	233 µrad

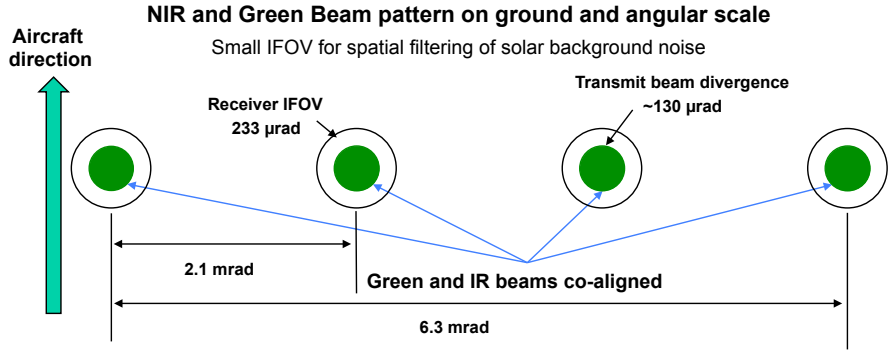

Figure 2. Geometry of SIMPL's four output beams spaced equally by 2.1 mrad spanning a 6.3 mrad swath in the cross track direction. Each beam projects a ~130 µrad spot on the ground with co-aligned wavelengths. The instantaneous field of view (IFOV) of the receiver is ~233 µrad per beam. *Note: drawing not to scale.*

1.2 Laser Transmitter Subsystem

The laser transmitter is a passively Q-switched microchip laser from Teem Photonics (model SNP-08E-OEM) with a pulse repetition frequency (PRF) at ~11 kHz and ~6 µJ of output pulse energy (average power ~70 mW) at 1064 nm. The output beam of the microchip laser is TEM_{00} with a full beam divergence at $1/e^2$ of 12 (Horizontal) x 14 (Vertical) mrad. The laser transmitter layout is shown in Figure 3.

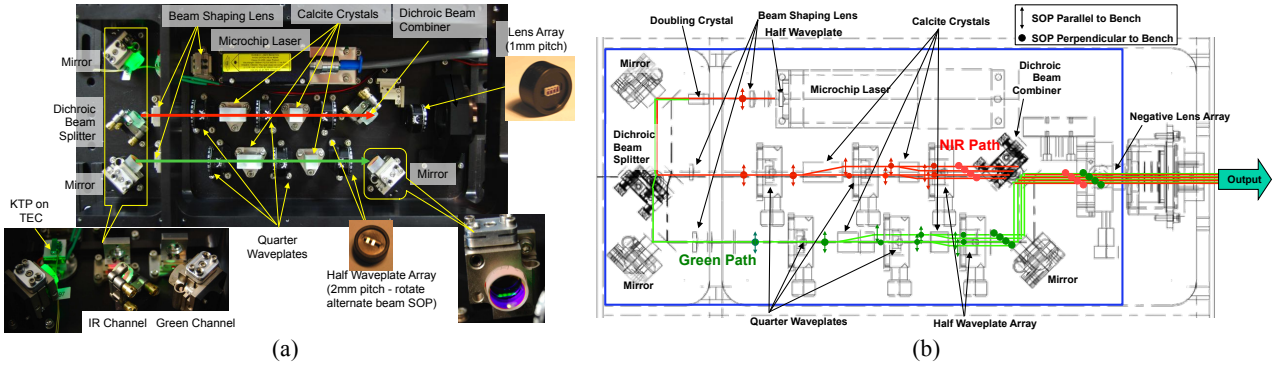

Figure 3. (a) Photograph of the SIMPL laser transmitter showing the separation of the NIR and Green optical paths after the doubling crystal using a dichroic splitter. On each path four beams with parallel polarization are produced using calcite beam separators and waveplates. The beams are then recombined with a dichroic combiner with the two colors co-aligned prior to final beam shaping optics to meet the beam divergence requirement. The lower right hand corner shows the four beams on the green wavelength path prior to recombining with the NIR. (b) The figure shows the polarization beam trace through the system. The output transmit SOP for both colors are perpendicular to the optical bench.

As seen in Figure 3 (a) and (b) a doubling crystal is used to convert a portion of the 1064 nm output to 532 nm. The frequency doubling is done using a Type II non-critically phase matched KTP crystal that is temperature controlled using a thermal electric cooler (TEC). Temperature control of the KTP crystal determines the doubling efficiency that allows for real-time adjustments of the NIR/Green conversion ratio (from 5% to ~37% over ΔT ~40 degrees) during the airborne flights. A dichroic beam splitter divides the two colors into separate optical paths. After the splitter beam shaping lenses establish the beam divergence of ~130 µrad for both colors. Following the beam shaping lenses a portion of the energy on each path is reflected vertically and exits the transmitter enclosure through three apertures on the laser transmitter cover. The purpose of these pick-offs are described in the Section 1.3. On each optical path a sequence of waveplates and birefringent calcite crystals produce four beams which all have the same polarization plane. The first quarter waveplate generates circularly polarized light from the plane polarized transmit beam which is then split by the first calcite crystal into parallel and perpendicular components forming two beams with equal intensities. The calcite crystal length defines the physical pitch of 2 mm between the beams. The second quarter waveplate circularly polarized the incident plane polarized beams and then the second, shorter calcite crystal splits the two beams into the two polarization components, forming four beams with equal intensities and a pitch of 1 mm between beams. For each wavelength, a waveplate array with half waveplates on a 2 mm pitch rotates the alternate beam polarization planes by 90° so that all beams have the same SOP with the polarization plane oriented perpendicular to the optical bench. A second dichroic optic recombines the two colors that are co-aligned in each beam. A 4-lens array establishes the 2.1 mrad beam-to-beam divergence. A polarizing beam splitter is used as a final step to ensure ≥ 100:1 polarization contrast ratio.

After passing through the polarizing beam splitter, the transmit beams reflect off of a small folding mirror. The folding mirror directs the beams perpendicularly to the secondary mirror that reflects the beams to the 20 cm diameter primary mirror. That mirror reflects the beams at nadir to the surface. Upon exit from the instrument the beams are overlapping with a combined diameter of 70 mm and 5 mm beam-to-beam separation. The nominal ocular hazard distance (NOHD) of the combined beams and colors is 0 m and is therefore eye safe. The diverging beams become fully separated at a distance of 23 m.

1.3 Transmit Echo Pulse, Start Pulse Detector and Power Meter

As mentioned previously, pick-off optics are placed along the transmitter optical paths to direct laser pulse energy vertically out of the transmitter enclosure through three apertures. This pulse energy is used for three purposes. Light from the first pick-off, located on the NIR path after the dichroic, enters a start pulse detector to provide pulse events to the receiver electronics that are used as the starting time of the photon round-trip travel time measurement. The two wavelength paths also have pick-off optics for power monitoring and for capturing the transmit echo pulse (TEP). For each wavelength, light enters a beam splitter cube that directs part of the light for power monitoring and a portion of the light is directed to the TEP collection lenses. The TEP optics are used to record the instrument impulse response pulse

shape which is the convolution of the transmit pulse shape and the receiver pulse broadening. As seen in Figure 4, individual single mode fibers transmit the energy through couplers to 34 m fiber spools that delay the pulses to separate them in time from internal scattered light signals. The delay fibers are coupled to fibers that transmit the pulses to projection lenses that disperse the light into the primary mirror. This light follows the full receive path to record the impulse responses on the sixteen channels using the same optics, SPCM detectors and electronics as the pulses reflected from the surface. Deconvolution of the impulse response from the surface return provides a measure of pulse broadening due to surface roughness, slope and penetration.

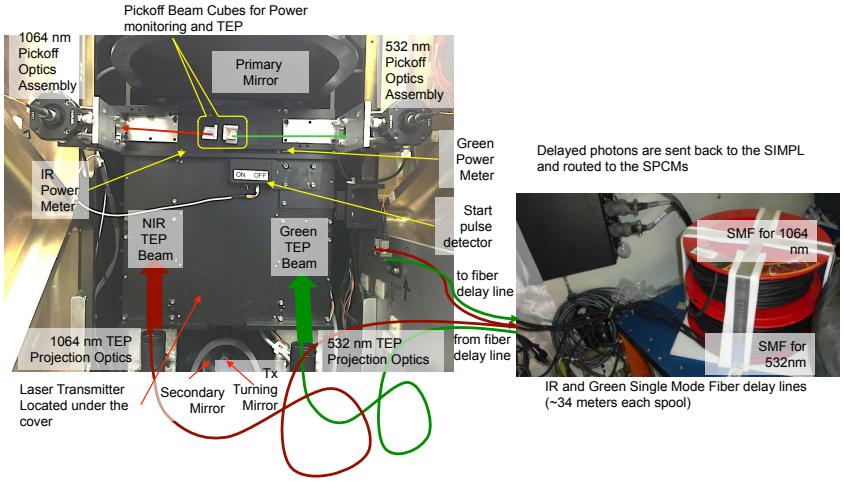

Figure 4. Layout of the pick-off optics for the start pulse, power monitoring and TEP capture in the SIMPL instrument.

1.4 Receiver Subsystem

The return signal is captured by the instrument's 20 cm OAP aperture. Upon entry a small portion of the return laser energy is obscured by the back of the secondary mirror assembly. The remaining energy is collected by the primary mirror and reflected to the secondary mirror. The light is directed vertically through an opening in the optical bench and enters a folding mirror assembly that reflects the light horizontally to a pin-hole field stop (Figure 6(a) and (b)). The field stop consists of four pinholes that define the 233 µrad field of view (FOV) for each beam. The small FOVs are used to spatially reject solar background photons. A lens array follows that collimates the incoming beams and a dichroic beam splitter divides the two colors into separate optical paths.

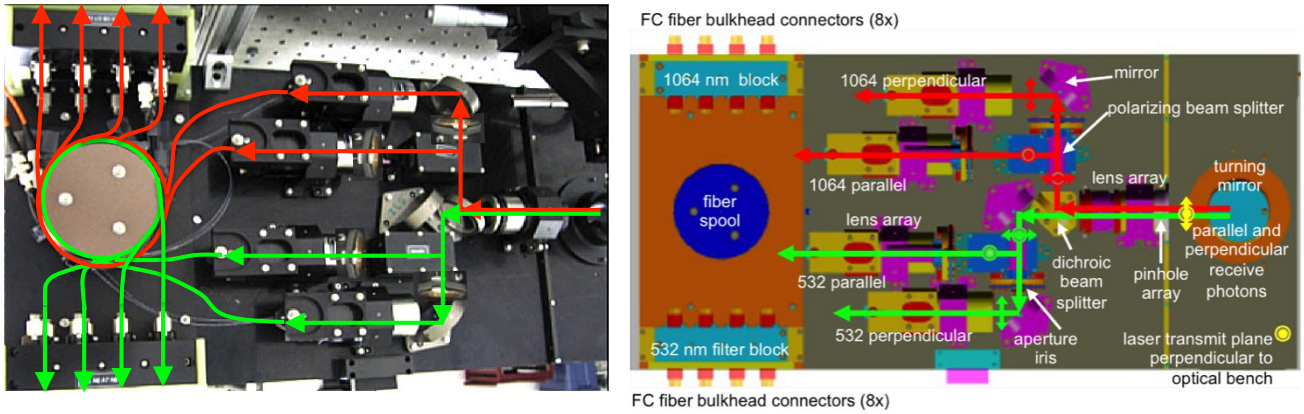

(a) (b)

Figure 5. (a) Photograph of the receiver subsystems with the lines showing the optical and fiber routing paths for the four color/polarization modes. (b) Schematic diagram of the receiver subsystem components with the SOP ray traced through the receiver paths for each color.

On each path a double stack of polarizing beam splitters separates the return energy into photons with polarization states that are parallel and perpendicular to the plane-parallel polarized transmit beams. The four color and polarization modes each pass through a mechanical iris that can be used to attenuate the beam energy (the irises were not installed on the bench at the time of the photo; insets have been added to show their location). Lens array assemblies for each of the four modes focus the beams into four fibers that have a 0.22 numerical aperture and 100 micron stepped index core size. Using a spool to reduce bending the fibers are coupled to 1064 nm and 532 nm filter blocks each of which consist of eight narrow-band spectral filter assemblies to reject out-of-band solar background photons. The filter assemblies are temperature controlled to maintain stable band pass wavelengths. Four thermistors are installed to record the temperature at two locations on each filter block using a four-channel data logger. On exit from the filter blocks 16 fibers, which have a 0.37 numerical aperture and 200 μm step-index core size, transmit the signals to four SPCM quad detectors in an adjacent instrument rack. The four signals for a beam are directed to one of the quad detector modules. The SPCM detection quantum efficiency is in the range 50 to 60% at 532 nm and 1.6 to 2.3% at 1064 nm. SPCMs were the only photon counting detectors available at the time of SIMPL's development with sensitivity in the NIR.

1.5 Electronics and Command and Data Handling (C&DH)

An electronics rack is used to house an enclosure containing the four quad SPCM modules as seen in Figure 6(a) and (b). The rack also houses a power supply enclosure, dual channel power meter and a doubling crystal temperature controller. The power supply enclosure contains three DC power supplies, a start-pulse discriminator, two 1 to 10 TTL fanout boards and front panel mounted voltage and current meters. The discriminator takes as input the signal from the laser fire start pulse detector. One fanout board takes this discriminator TTL output and produces duplicate laser fire pulses that go to four P7889 event timer interface boards, each of which has four channels. The other fanout board distributes the GPS 1 pulse per second (pps) signal to the four boards.

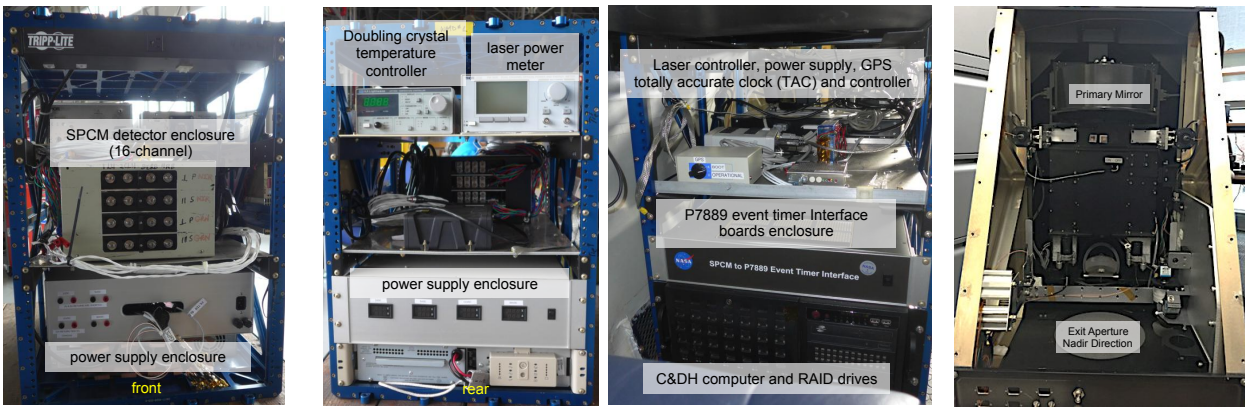

(a) (b) (c) (d)

Figure 6. (a) Front and (b) rear of the electronics rack, (c) front of the C&DH rack and (d) SIMPL transceiver mounted in its enclosure frame. A color frame camera is located in the lower right. A light shield covers the open side during operation.

The C&DH rack shown in Figure 6(c) houses the enclosure containing the event timer interface boards. Each board times the arrival of start pulse, GPS pps and photon events with 100 picosecond (1.5 cm) resolution. Each times the photon events for the four color/polarization channels on one beam. The relative arrival time of the events are defined by the CPU clock frequency. GPS absolute time is inserted into the timer event streams by the CPU provided by a totally accurate clock (TAC) that receives input from a dual-frequency GPS antenna. The computer issues commands to the instrumentation and stores the event arrival times on RAID drives. The rack also houses the CPU keyboard and screen and the laser controller and power supply. A laptop is used to run Applanix POS AV and power meter software. The Applanix instrument is mounted adjacent to SIMPL, providing position and attitude data used in geolocating the laser photon reflection points. The laptop also records nadir frame camera images that document the surface conditions.

2. MEASUREMENT RESULTS

2.1 Measurement Methods

SIMPL's measurements of photon round-trip travel times, converted to ranges, provide highly resolved information about surface elevation, roughness, slope and laser light penetration depth. Signal amplitudes (photon density) from the laser retro-reflectance and solar bi-directional reflectance (the background noise rate) on each of the 16 channels are sensitive to surface light scattering, providing unique information used to differentiate surface properties and types. For example, the amount of multiple-scattering at each wavelength is estimated using the ratio of the parallel and perpendicular signals, thereby measuring the depolarization of the plane-polarized transmit pulses and polarization of randomly polarized sunlight. Upon single scattering from a target the reflected laser energy remains parallel to that of the plane-polarized laser pulse. As multiple scattering increases the fraction of the energy converted to the perpendicular state increases. By adding the ranging component, building upon prior non-ranging measurements of laser depolarization at 355, 532 and 1064 nm,[4,5] SIMPL provides a vertical profile measurement of the depolarization ratio. This yields a means to investigate the height distribution of surface and volume multiple scattering in transmissive targets (snow, ice, water, vegetation) to better understand the interaction of pulsed laser energy with those targets. Volume multiple scattering increases photon travel path lengths thereby introducing a ranging bias error that erroneously lowers surface elevations if the bias is not accounted for.

Prior work using SIMPL data acquired over Lake Erie ice cover in 2010 demonstrated differentiation of open water, snow and several ice facies as well as differences in the depths of 532 nm laser pulse penetration.[6] The 1064 nm photon ranges provide a reference to the true surface elevation because the penetration depth is negligible at that wavelength. The co-incident wavelengths illuminate small footprints (0.3 m diameter) so that return pulse broadening due to surface slope and roughness is minimized in order to observe the ranging bias due to 532 nm penetration. Eight cm single photon range precision enables sub-cm level determination of penetration depth profiles using calibrated range histograms of pulse broadening. In addition SIMPL's measurement of laser return depolarization definitively identifies the presence of surface water due to the absence of the NIR and Green perpendicular polarization signals, aiding in the interpretation of the penetration results. Those signals are absent because water surfaces are specular, thereby undergoing only single scattering.

2.2 SIMPL Airborne Campaigns

SIMPL has flown on two multi-instrument airborne campaigns. During the 2011 Eco-3D campaign on the NASA P3-B SIMPL was flown with the Digital Beam forming SAR (DB-SAR)[7] and the multi-angle, multi-wavelength imaging Cloud Absorption Radiometer (CAR).[8] Data was collected at numerous Eastern U.S. long-term ecology study sites to assess simultaneous laser, radar and solar reflectance measurements of forest canopy vertical structure. In Northwest Greenland during July and August, 2015 SIMPL was flown over the ice sheet and sea ice along with a hyperspectral imager (AVIRIS-NG),[9] each on a dedicated King Air, for a total of 37 hours. This campaign was done to support NASA's upcoming ICESat-2 mission that will provide measurements of changing ice sheet elevations and sea ice thicknesses likely due to climate change. The mission's multi-beam ATLAS laser altimeter acquires pulsed, photon counting ranging data like SIMPL, but in large (12 m diameter) footprints and only at a 532 nm without the polarimetry capability. These measurements will not unambiguously determine penetration depths into snow, ice and water nor the resulting ranging biases. SIMPL's measurements will be used to quantify errors in ice sheet elevations and sea ice thicknesses as a function of grain size, contaminant concentration and wetness estimated using the AVIRIS-NG data. This information will help to understand changes in penetration depth due to seasonal and/or inter-annual variation in these properties that could result in errors in the ICESat-2 measured trends of ice sheet elevation and sea ice thickness.

An example of SIMPL data collected across a melt pond on the ice sheet is shown in Figure 7(a) for the 532 nm parallel and Figure 7(b) for the 1064 nm perpendicular signals. The absence of the perpendicular photons definitively identifies where surface melt water is present, as opposed to an ice covered or completely frozen pond. The 532 nm photons penetrate into the water column then reflect from the pond bottom, providing a measurement of the pond depth along the profile. Figure 8 shows data acquired over Nares Strait sea ice. The frame camera image shows a network of melt water channels on the ice. The absence of NIR and green perpendicular signals from the surface identifies the locations of that water. Beneath the water and ice the density of 1064 nm photons is not greater than the solar background rate indicating no laser pulse volume scattering was detected, as expected. The increased density of 532 nm photons below the surface

provides a depth profile measurement of single and multiple-scattering within the ice and water. The histogram shapes are broadened due to surface slope and roughness. The surface slope is due to an aircraft roll effect, which is not removed in this range data. The laser after pulse is prominent in the NIR and reduced in amplitude in the green.

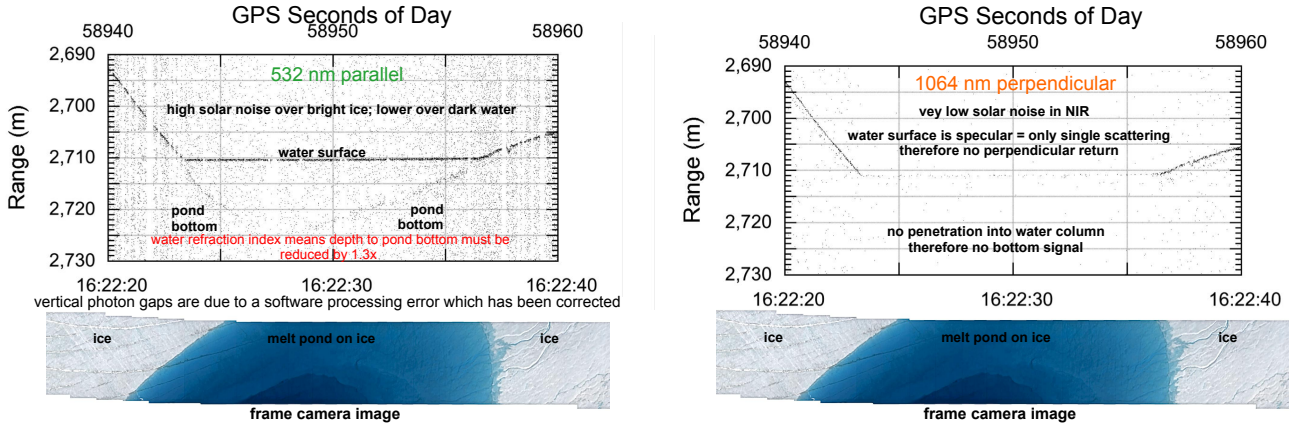

Figure 7. SIMPL "point cloud" plots, for one of the four beams, of single photon returns across a melt pond in the Greenland coastal ice sheet ablation zone. The correlated returns are from the ice and water surfaces. The uniform background "noise" photons are from sunlight reflected continuously from the surface. The image, from the frame camera operating simultaneously with SIMPL, documents the surface conditions.

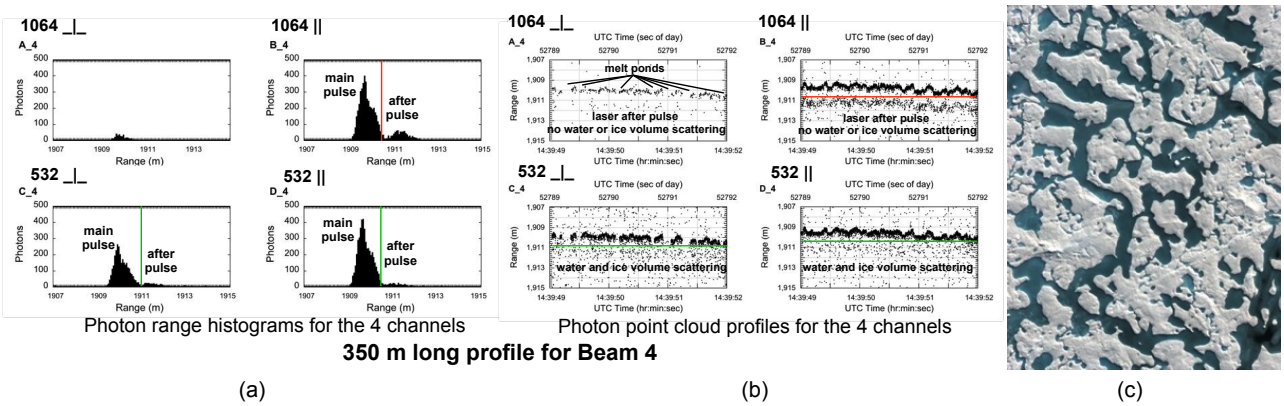

Figure 8. SIMPL data showing the perpendicular (_|_) and parallel (||) components of the NIR and green returned signals for one of the four beams. The data shows (a) photon range histograms; (b) photon point clouds; and (c) frame camera image of Nares Strait sea ice with a melt water network on the surface.

3. CONCLUSIONS

The airborne four-beam SIMPL lidar was developed with funding from the NASA Earth Science Technology Office (ESTO) Instrument Incubator Program (IIP) in order to demonstrate advanced altimetry measurement capabilities. Beginning in 2008 a series of flight missions were successfully executed and valuable two color data on depolarization due to surface optical scattering properties have been studied and documented. In addition to the altimetry height data the amplitudes of the laser pulse retro-reflectance and solar bi-directional reflectance are measured on 16 channels. The SIMPL instrument is ideally suited to quantify green laser pulse penetration depths into snow, ice and water. It also definitely identifies the presence and depth of melt ponds on ice sheets and sea ice. Flights during July and August, 2015 in northwest Greenland collected data for a wide range of surface types in preparation for the launch of NASA's ICESat-2 mission in late 2017. A Transmit Echo Pulse capability was added for the Greenland campaign to measure the instrument impulse responses on each channel that are needed to quantify pulse broadening due to surface slope, roughness and penetration.

ACKNOWLEDGEMENTS

The authors acknowledge support from the NASA's ESTO program and ICESat-2 Project Science Office. Susan Valett, Kurt Rush and Beth Timmons are team members at NASA Goddard Space Flight Center who contributed to the development and operation of SIMPL. Gerry McIntire and Ray Desilvester provided mechanical support. Sigma Space Corporation participated in the design and integration of the instrument.

REFERENCES

[1]. Dabney, P., D. Harding, J. Abshire, T. Huss, G. Jodor, R. Machan, J. Marzouk, K. Rush, A. Seas, C. Shuman, X. Sun, S. Valett, A. Vasilyev, A. Yu, and Y. Zheng, "The Slope Imaging Multi-polarization Photon-counting Lidar: development and performance results," Geoscience and Remote Sensing Symposium, 2010 IEEE International, DOI10.1109/IGARSS.2010.5650862, 253-256 (2010). See also https://directory.eoportal.org/web/eoportal/airborne-sensors/simpl

[2]. Abdalati, W., H.J. Zwally, R. Bindschadler, B. Csatho,S.L. Farrell, H.A. Fricker, D. Harding, R. Kwok, M. Lefsky, T. Markus, A. Marshak, T. Neumann, S. Palm, B. Schutz, B. Smith, J. Spinhirne and C. Webb, "The ICESat-2 laser altimetry mission," Proceedings of IEEE, 98, 5, 735-751 (2010). See also, http://icesat.gsfc.nasa.gov/icesat2/

[3]. McGill, M., D. Hlavka, W. Hart, V. S. Scott, J. Spinhirne and B. Schmid, "Cloud Physics Lidar: instrument description and initial measurement results," in Applied Optics, 41, 18, 3725-3734 (2002). See also, http://cpl.gsfc.nasa.gov

[4]. Kalshoven, Jr., J.E. and P.W. Dabney, "Remote sensing of the Earth's surface using an airborne polarized laser," IEEE Transactions Geoscience and Remote Sensing, 31, 438–446 (1993).

[5]. Kalshoven, Jr., J.E., M.R. Tierney, Jr., C.S. T. Daughtry and J.E. McMurtrey III, "Remote sensing of crop parameters with a polarized, frequency-doubled Nd:YAG laser," Applied Optics, 34, 2745- 2749 (1995).

[6]. Harding, D., P. Dabney, S. Valett, A. Yu, A. Vasilyev and A. Kelly, "Airborne polarimetric, two-color laser altimeter measurements of lake ice cover: A pathfinder for NASA's ICESat-2 spaceflight mission," Geoscience and Remote Sensing Symposium (IGARSS), 2011 IEEE International, DOI 10.1109/IGARSS.2011.6050002, 3598-3601, (2011).

[7]. Rincon, R.F., T. Fatoyinbo, J. Ranson, G. Sun, M. Perrine, Q. Bonds, S. Valett, S. Seufert, "Digital Beamforming Synthetic Aperture Radar (DBSAR) polarimetric operation during the Eco3D flight campaign," Geoscience and Remote Sensing Symposium (IGARSS), 2012 IEEE International, doi: 10.1109/IGARSS.2012.6351101, 1549-1552 (2012). See also, https://directory.eoportal.org/web/eoportal/airborne-sensors/dbsar

[8]. Roman, M.O., C. K. Gatebe, C. Schaaf, R. Poudyal, Z. Wang, M. D. King, "Variability in surface BRDF at different spatial scales (30 m–500 m) over a mixed agricultural landscape as retrieved from airborne and satellite spectral measurements," Remote Sensing of Environment, doi:10.1016/j.rse.2011.04.012, 115, 2184-2203 (2011). See also, http://car.gsfc.nasa.gov

[9]. Dozier, J. and T.H. Painter, "Multispectral and hyperspectral remote sensing of alpine snow properties," Annual Review of Earth and Planetary Sciences, 32, 465-494 DOI: 10.1146/annurev.earth.32.101802.120404 (2004). See also, http://avirisng.jpl.nasa.gov.